scientific reports

Check for updates

OPEN

Microbe cultivation guidelines to optimize rhamnolipid applications

Ilona E. Kłosowska-Chomiczewska[1]✉, Adam Macierzanka[1], Karol Parchem[2], Pamela Miłosz[1], Sonia Bladowska[1], Iga Płaczkowska[1], Weronika Hewelt-Belka[3] & Christian Jungnickel[1]

In the growing landscape of interest in natural surfactants, selecting the appropriate one for specific applications remains challenging. The extensive, yet often unsystematized, knowledge of microbial surfactants, predominantly represented by rhamnolipids (RLs), typically does not translate beyond the conditions presented in scientific publications. This limitation stems from the numerous variables and their interdependencies that characterize microbial surfactant production. We hypothesized that a computational recipe for biosynthesizing RLs with targeted applicational properties could be developed from existing literature and experimental data. We amassed literature data on RL biosynthesis and micellar solubilization and augmented it with our experimental results on the solubilization of triglycerides (TGs), a topic underrepresented in current literature. Utilizing this data, we constructed mathematical models that can predict RL characteristics and solubilization efficiency, represented as $logP_{RL} = f$(carbon and nitrogen source, parameters of biosynthesis) and $logMSR = f$(solubilizate, rhamnolipid (e.g. $logP_{RL}$), parameters of solubilization), respectively. The models, characterized by robust R^2 values of respectively 0.581–0.997 and 0.804, enabled the ranking of descriptors based on their significance and impact—positive or negative—on the predicted values. These models have been translated into ready-to-use calculators, tools designed to streamline the selection process for identifying a biosurfactant optimally suited for intended applications.

Keywords Biosurfactant design, Rhamnolipid biosynthesis, Micellar solubilization, Microbial cultivation, QSPR

Abbreviations

BS	Biosurfactant
CMC	Critical micellar concentration
*log*P	Logarithm of octanol–water partition coefficient
MSR	Molar solubilization ration
MV	Molecular volume
RL	Rhamnolipid
TB	Tributyrin
TG	Triglyceride
TO	Triolein

Microbial surfactants, a subgroup of biosurfactants (BSs) primarily represented by rhamnolipids (RLs), are garnering increasing attention for their potential in various applications. They are widely recognized for being skin-friendly[1,2], non-toxic[3], and readily biodegradable[3,4]. Consequently, they are frequently studied to gain a deeper understanding of their behaviour in aqueous solutions under different conditions[5] and for numerous application purposes[6,7]. Despite having been studied since the 1950s, there remain significant gaps in the field of BS science that warrant further investigation. This study addresses two primary knowledge gaps: I. the applicational properties, specifically micellar solubilization, and II. a targeted synthesis approach for BS research, described further in more detail.

[1]Department of Colloid and Lipid Science, Faculty of Chemistry, Gdańsk University of Technology, 11/12 G. Narutowicza St., 80-233 Gdańsk, Poland. [2]Department of Chemistry, Technology and Biotechnology of Food, Faculty of Chemistry, Gdańsk University of Technology, 11/12 G. Narutowicza St., 80-233 Gdańsk, Poland. [3]Department of Analytical Chemistry, Faculty of Chemistry, Gdańsk University of Technology, 11/12 G. Narutowicza St., 80-233 Gdańsk, Poland. ✉email: ilochomi@pg.edu.pl

The exploration of the first aspect, i.e. micellar solubilization, seems somewhat incomplete given the myriad combinations of solubilizate and BS. A meticulous review of research papers published since 1995 yielded only 28 publications that provided complete or semi-complete numerical descriptions of the solubilization process in the form of a molar solubilization ratio (MSR). The MSR is the metric most commonly used to describe micellar solubilization efficiency across all surfactants[8]. No reports older than 27 years were identified. A brief analysis of the juxtaposed metadata (SI, "MSR dataset") suggests that RL solubilization capacities predominantly pertain to compounds with environmental applications. For instance, n-alkanes were featured in 9, and aromatics in 15 of the 28 examples. There is a conspicuous absence of research on solubilization relevant to household contexts (e.g., handwashing, dishwashing), as well as the pharmaceutical or cosmetic industries (such as oil-soluble vitamin supplements or cosmetic emulsions). This research gap might be bridged by undertaking experiments with triglycerides (TGs), which are the primary constituents of vegetable oils.

The second issue, i.e. targeted biosynthesis, is no less significant. Much of the BS research seems to adopt a bottom-up approach. In such a method, research groups identify potential applications for a previously synthesized and analyzed BS, tailoring these applications to the known properties of BSs, rather than the reverse[9–12]. In response to that, we previously proposed a top-down approach for BS. In this strategy, we employed the quantitative structure–property relationship (QSPR) to select BSs with the desired properties for specific targeted applications[8,13]. Our research yielded models that can predict the CMC or MSR of RLs best suited for a chosen solute. Analyzing such models helps in identifying the optimal BS for a given application. Targeted synthesis requires, however, an in-depth and accurate understanding of how selected biosynthesis parameters (e.g., carbon source, nitrogen source, C:N ratio, pH, temperature, etc.) influence BS composition. Typically, such determinations are made to maximize yield[14–19], with only occasional emphasis on how the parameters affect the final product's composition. For instance, Nitschke et al.[20] illustrated how the hydrophilicity of a carbon source impacts the composition of the RL mixture produced by *Pseudomonas aeruginosa* LBI. When cultivated on hydrophobic oil wastes, there was a predominance of monorhamnolipid (monoRL). Similarly, Nicolo et al.[21] found that *Pseudomonas aeruginosa* PAL05 primarily produces monoRL when grown on substrates providing long-chain fatty acids, such as *Brassica carinata* oil or myristic acid, and dirhamnolipid (diRL) when using glycerol or glucose as the carbon source. Santos et al.[15] demonstrated that cultivating *Pseudomonas aeruginosa* with different combinations of nitrogen and carbon sources could vary the monoRL and diRL contents in the final product, ranging between 14–67% and 33–85%, respectively. In another study, Santos et al.[22] revealed that pH not only affects the efficiency of RL production by the *Pseudomonas aeruginosa* PA1 strain but also the mono- to diRL ratio in the final product. Conversely, Costa et al.[23] and de Santana-Filho et al.[24] established that the RL congener distribution evolves over the cultivation period, respectively for *Burkholderia glumae* AU6208 and *Pseudomonas aeruginosa* UFPEDA. Both the efficiency of biosynthesis and the congener diversion are influenced by the sulphur source, as Ismail et al. [25] found in RL production by *Pseudomonas aeruginosa* AK6U. While these studies offer invaluable insights, they are relatively limited and often restricted to specific microbial species.

A comprehensive meta-analysis, systematic organization, and statistical evaluation of broader RL production data could simplify the selection of biosynthesis conditions. Moreover, integrating such meta-analysis data with application-specific data could potentially serve as a tool for producing surfactants with tailored properties. While there are examples of applying chemometric tools in RL research, they mainly focus on optimizing BS production efficiency[26–28], aggregation behavior[29], solubilization and biodegradation of PAHs[30], treatment of oily sludges[31,32], coal recovery[33], and selected adsorption characteristics[34]. To our knowledge, attempts of developing guidelines for the biosynthesis of BSs with specified and targeted properties have not been reported in the scientific literature so far.

Considering all the aforementioned points and aiming to provide a more comprehensive view of BS science, we hypothesized that by generating new experimental data on solubilization of TGs, integrating it with existing literature data on solubilization and biosynthesis, and employing selected chemometric tools, it is possible to formulate a computational blueprint for the biosynthesis of RLs with specific application-oriented properties. Therefore, we aimed at delivering mathematical models to predict (i) the composition of the RL biosynthesized at fixed conditions, and (ii) the efficiency of the obtained RL as a solubilizing agent. We have then transformed the models into ready-to-use calculators for facilitating the biosynthesis of RLs with customized properties.

Materials and methods

Materials

The RL preparation R90 was purchased from Agae Technologies (USA). It is a powdered BS containing 90% of RLs with monoRL to diRL ratio 3:2 (w/w). The R90 was used as a source of monoRLs and diRLs. TB (97%, Sigma-Aldrich, W222305) and TO (≥ 99%, Sigma-Aldrich, T7140) were used as solubilizates in solubilization experiments.

Chloroform, methanol, and isopropanol (all ≥ 98.5%) for column chromatography were purchased from POCh (Gliwice, Poland). Gradient grade isopropanol (1.01040), methanol (1.06007), hexane (1.03701) and acetonitrile (1.00030) for HPLC analysis were purchased from MerckKGAA (Darmstadt, Germany). Ammonium formate (98%), sodium azide, sodium hydroxide and Hydrochloric acid were obtained from Chempur (Krupski Młyn, Poland).

Biosurfactant stock solution was prepared in redistilled water (Hydrolab, Straszyn, Poland) with 0.02% (w/w) NaN_3. Biosurfactant solutions were prepared by serious dilution of the stock solution. Sodium hydroxide and hydrochloric acid solutions were used for pH adjustment.

Separation of RLs

We used the purchased R90 preparation as a source of RLs, and separated mono- and diRLs with preparative column chromatography. Silicagel (15-40 µm, Merck 60) was activated (105 °C, 3 h) and suspended in chloroform. Glass column (50 cm length, Φ 2 °cm) with a sinter was filled with the silica gel suspension. Subsequently, 2.5 g of BS was dissolved in chloroform and loaded into the column. The elution of RLs was performed according to Sim et al.[35]. Briefly, neutral lipids were eluted with ca. 500 mL of chloroform, monoRLs were eluted with ca. 1000 mL of chloroform/methanol (50:3 v/v) followed by 200 mL of chloroform/methanol (50:5 v/v), and diRLs were eluted with ca. 300 mL of chloroform/methanol (50:50 v/v). Eluate fractions were collected in glass vials (10 mL each) at a flow rate 0.5 mL/min, regulated with a membrane pump (APR150, Aqua EL, Suwałki, Poland).

The composition of eluate fractions was analysed using TLC and HPLC Q-TOF methods, and fractions containing either monoRLs or diRLs were combined. The solvents were evaporated using a rotary evaporator (55 °C, 30 min), and the RL congeners obtained that way were further used for solubilization experiments.

RL separation efficiency assessment

The column chromatography eluate fractions were assessed with thin layer chromatography (TLC) and HPLC coupled to hybrid quadrupole-time of flight analyzer (Q-TOF).

For TLC, eluate fractions of 5 µL were spotted on silica gel plates (TLC 60 F_{254}, Merck, Poland). The chromatograms were developed in the ascending mode in a cylindrical developing chamber containing chloroform/methanol/water (65:15:2 v/v/v) under saturated conditions[35]. The spots were visualized by spraying the TLC plate with 10% phosphomolybdic acid in methanol and heated to 100 °C on the heating plate.

The MS analyses were performed using Agilent 1290 LC system equipped with a binary pump, online degasser, autosampler, and a thermostated column compartment, coupled to a 6540 Q-TOF–MS with a dual electrospray ionization (ESI) source (Agilent Technologies, Santa Clara, CA, USA). The extracts were injected directly to the ion source. The mobile phase consisted of 50% 10 mM ammonium formate/methanol (10:90 v/v) (component A) and 50% hexane/isopropanol/5 mM ammonium formate (20:79:1 v/v/v) (component B). The mobile phase flow rate was set to 0.5 mL/min. The injection volume was 2 µL. The ESI source was operated in the positive ion mode with ion spray voltage 120 V. Data were collected using SCAN acquisition mode in a range from 100 to 2200 m/z in high-resolution mode (4 GHz). MS analysis parameters included a capillary voltage of 3500 V, fragmentation voltage of 120 V, nebulizing gas at 35 psi, and a drying gas temperature of 300 °C. Mono- and diRLs were monitored by 522.3636 and 668.4215 m/z ($[M^+NH_4]^+$ adducts), respectively[36].

Solubilization experiments

RL solutions of different concentrations were prepared by a serial dilution of a stock solution. Solubilization was carried out in glass vials (10 mL) with an aperture at the bottom, sealed with silicone septa. Biosurfactant solution (2.5 mL) was transfered into the vial and oil phase (i.e., TB or TO) was added in excess (0.25 mL). Vials were closed with a cap sealed with Teflon septa and mixed thoroughly (1000 rpm, 24 h, 25 °C) using a horizontal shaker (IKA VIBRAX VXR Basic, Sigma-Aldrich) in order to allow for incorporation of oil phase into BS micelles. Subsequently, the excess oil phase was separated by centrifugation at 5000 rpm for 15 min (MPW-350 Med. Instruments, Poland). Immediately after the centrifugation, 1 mL of clear bottom phase was collected with a syringe through silicone septa and stored at 4 °C prior to further analysis. All the solubilization experiments were performed in triplicate.

Solubilization efficiency assessment

The concentration of TB or TO solubilized in RL micelles was analyzed by reverse phase (RP) UHPLC using Dionex UltiMate 3000 equipped with Corona Veo RS and UV–VIS/DAD detectors, kindly provided by Polygen (Gliwice, Poland). The MSR values of solubilizates were assessed from the slope of the solubility curves above the CMC of BS [37,38].

Solubilization of TB

Zorbax Bonus RP column (150 × 1.8 mm, 5 µm, Agilent Technologies, USA) was used for the separation of micellar phase components. The mobile phase used for the determination of TB consisted of 5 mM ammonium formate (component A) and acetonitrile (component B). The following gradient elution programme was used: a linear increase of B from 5 to 80% within 4 min, followed by 80% B maintained for 9.5 min. Then, the column was equilibrated for 3 min with 5% B. The flow rate of the mobile phase was 800 µL/min, and the injection volume was 10 µL. The column temperature was maintained at 40 °C throughout the separation process.

Solubilization of TO

Poroshell 120 EC-C8 column (100 × 2.1 mm, 2.7 µm, Agilent Technologies, USA) was used for the separation of micellar phase components. The mobile phase used for the determination of TO consisted of water (component A), acetonitrile (component B), and isopropanol (component C). The gradient elution programme was as follows: a linear increase of B from 5 to 95% within 5 min, followed by a simultaneous linear decrease of B to 0%, and an increase of C from 0 to 95% within 5 min. Next, 0% B and 95% C were maintained for 5 min. Subsequently, the column was equilibrated with 5% B and 0% C for 5 min. The flow rate of the mobile phase was 1 mL/min, and the injection volume was 5 µL. The column temperature was maintained at 40 °C throughout the separation process.

CMC determination

The pendant drop technique was used to assess the CMC of RL solutions (DSA 10, Krüss, Germany). The tensiometer was calibrated each time before using a RL solution by measuring the surface tension of redistilled water. The solutions used for the assessment of CMC were prepared by serious dilutions of the RL stock solutions that were also used for the solubilization studies. Redistilled water was used to dilute a stock solution to the concentrations required. The equilibrium surface tension measurements were performed at 25 °C. All the measurements were run at least in triplicate. The isotherms of surface tension vs the logarithm of BS concentration were plotted and the CMC was determined from the intersection of two lines, i.e. before and after reaching the plateau of surface tension. The CMC data were further used for the purpose of modeling the efficiency of solubilization in RL solutions, where CMC served as one of the descriptors of the BS.

Literature data collection for databases

Google Scholar was used for literature data collection as it provides high coverage of published research data[39]. *Rhamnolipid, rhamnolipid production, relative abundance*, *rhamnolipid solubilization, rhamnolipid MSR*, *rhamnolipid WSR,* and *rhamnolipid molar solubilization ratio* were used as keywords. The years 2009–2022 were covered in the search. Only two types of original papers were considered, i.e. publications providing full (continuous) data, and those providing data discontinuous only to the extent, where simple, literature-based assumptions could make them more or fully continuous. Publications giving precise BS composition (i.e. shares of RL homologs) and/or microbiological feed source composition were considered fully continuous and were used without additional calculational interventions. Publications providing discontinuous but still valuable information were supported with some simple assumptions. For example, when authors stated that BS contained 25.65% of monoRL and 74.35% of diRL[22], without specifying homologs, an average weighted RL composition was calculated for Rha-C10-C10 (one rhamnose and two residues of 3-hydroxydecanoic acid groups) and Rha-Rha-C10-C10 (two rhamnose moieties and two residues of 3-hydroxydecanoic acid groups) as the most abundant mono- and di-RL homologs[40,41]. In turn, when mono- and diRL congeners were given but without pointing monoRL/diRL ratio—like, for example, in the work by Thio et al.[42]—an average 35/65 ratio was assumed as it has been suggested in other studies on RLs[43–45]. Some further assumptions regarding, for example, the use of mixed carbon or nitrogen sources are presented in the Supplementary Information (SI, "RL production dataset"). As a result, data from 75 original publications[21–25,41,42,45–112] were used for creating the RL production database, resulting in 213 unique data points (SI, "RL production dataset"). For the purpose of creating the MSR database, data from 27 original publications were used[8,13,56,113–135] (57 literature data points, some of which were used in our previous report[8]) as well as additional original experimental data created for this study (17 data points), resulting in a total number of 74 data points (SI, "MSR dataset"). For modeling purposes, the process of BS synthesis was described by the following descriptors: carbon concentration, the molecular volume of carbon source (MV_C), the logarithm of octanol–water partition coefficient (*log*P), the concentration of nitrogen, carbon to nitrogen ratio (C:N, w/w), pH of the bacterial medium, incubation temperature and time, shaking speed (V, rpm). RLs were characterized by the logarithm of octanol–water partition coefficient $logP_{RL}$, CMC, and Impurity scale (0–5)[8,13], whereas the solubilization process was characterised by the molecular volume and the logarithm of octanol–water partition coefficient of solubilizate (MV_{SOL} and $logP_{SOL}$, respectively), pH, temperature (T), and the efficiency of the process expressed as MSR. Structural descriptors of carbon source and BS (i.e. MV and *log*P) were calculated as weighted average for the components/congeners using Molinspiration (Molinspiration Cheminformatics, Slovak Republic)[136].

When analysing the overall data, 9.6% of the data for the RL production (most commonly pH, followed by shaking speed and time of cultivation), and 1.99% of the data points for the MSR determination (most commonly pH, and temperature) contained missing data. Since the missing data was less than 10% it was decided to use Multivariate Imputation by Chained Equations (MICE) to estimate the missing data. The methodology has been described in detail in Łozińska et al.[137].

Computational modelling

An evolutionary algorithm (EA) was used to build the QSPR model by fitting a function to the provided data. For this purpose, GeneXproTools software (v5.0.3926, GepSotf, Portugal) was used. Each dataset was split randomly 80:20 into a training and a validation set, respectively. Three repetitions of each random split were conducted and calculated separately. Each calculation was repeated ten times. Root mean squared error (RMSE) was used as the fitting function. Both the $logP_{RL}$ and MSR were calculated. For calculations of $logP_{RL}$, the following descriptors were used—(i) bacterial feedstock characteristics: concentration of carbon mg/L, *log*P of carbon source, the concentration of nitrogen (mg/L), C:N ratio, and (ii) culture conditions: pH, temperature, shaking speed (rpm), and time of cultivation. For MSR prediction, the following were used: impurity scale (as described previously[8,13]), *log*P of the BS, *log*P of the solubilizate, the molecular volume of the solubilizate (nm^3), and CMC of the BS, as well as the temperature and pH of the solubilization process.

Statistical analysis

The analysis of the importance of each considered descriptor was performed with GeneXproTools software (v5.0.3926, GepSotf, Portugal). Any positive or negative impact of a descriptor on the predicted value was assessed as described previously[12]. Positive contribution (%) was assigned to data points where $\partial CMC/\partial x > 0$, and negative contribution (%) where $\partial CMC/\partial x < 0$.

Results and discussion

Computational modelling of RL production database

For the purpose of creating task-specific BS, we have first created a general model to describe the influence of carbon and nitrogen sources and the conditions of biosynthesis on the type of the RL product characterized numerically by its *log*P. This is referred to as the 'RL biosynthesis model' throughout the manuscript (Fig. 1). The general RL biosynthesis model was based on all collected data. The model was characterized by a good coefficient of determination R^2 of 0.608 (Fig. 2A). In the second approach, we aimed to analyze the effect of RL producers separately. This was because the cultivation conditions, the metabolic pathways, etc., may vary substantially between different types of RL-producing microbes, which can secrete different RL products. Therefore, we created separate models for the most represented groups of producers, i.e., *Pseudomonas* and *Burkholderia* species (Fig. 2B,C). The coefficient of determination obtained for the RL biosynthesis model for *Pseudomonas* species was slightly lower (R^2 0.581) than for the general RL biosynthesis model, indicating that *Pseudomonas* strains were too varied to be characterized by the descriptors widely available in literature data. On the other hand, a very satisfying R^2 of 0.997 was obtained for the RL biosynthesis model for *Burkholderia* species. This may indicate that the descriptors that were chosen for modeling RL production database describe differences between *Bulkholderia* strains well, or that the *Burkholderia* strains were less varied than the *Pseudomonas* strains. All three RL biosynthesis models were analyzed towards the importance of model descriptors (Fig. 2D). In general, descriptors of carbon and nitrogen source were the most important in all the models created, with *log*P of carbon

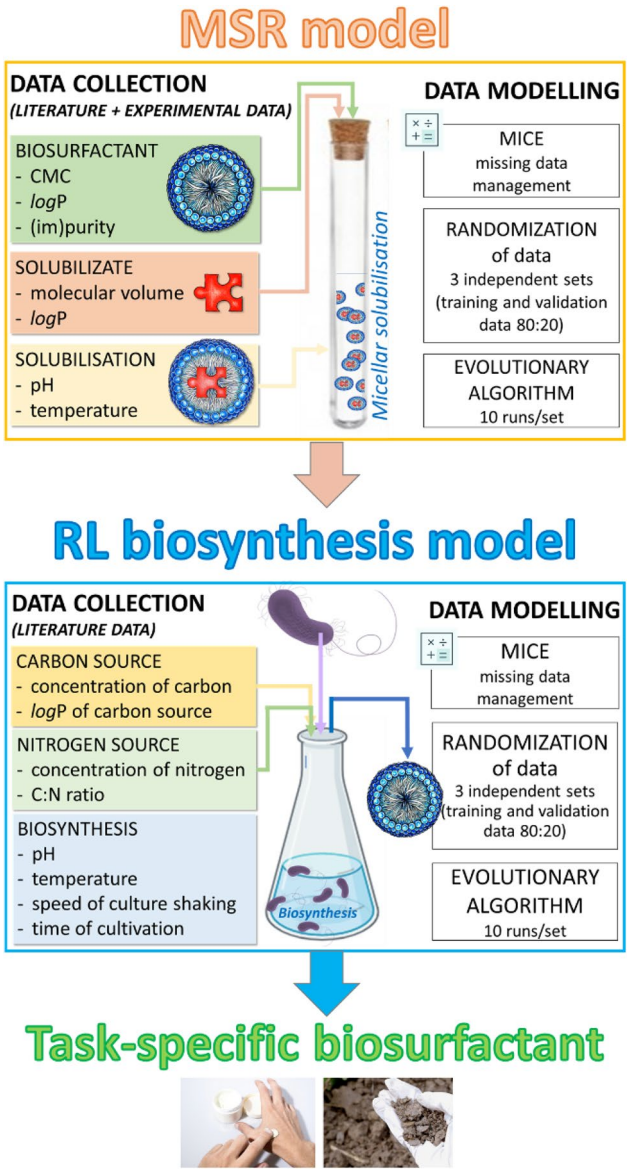

Figure 1. Workflow diagram for creation of RL biosynthesis and MSR models. The diagram also summarizes the way in which the models were used to define a recipe for a task-specific BS.

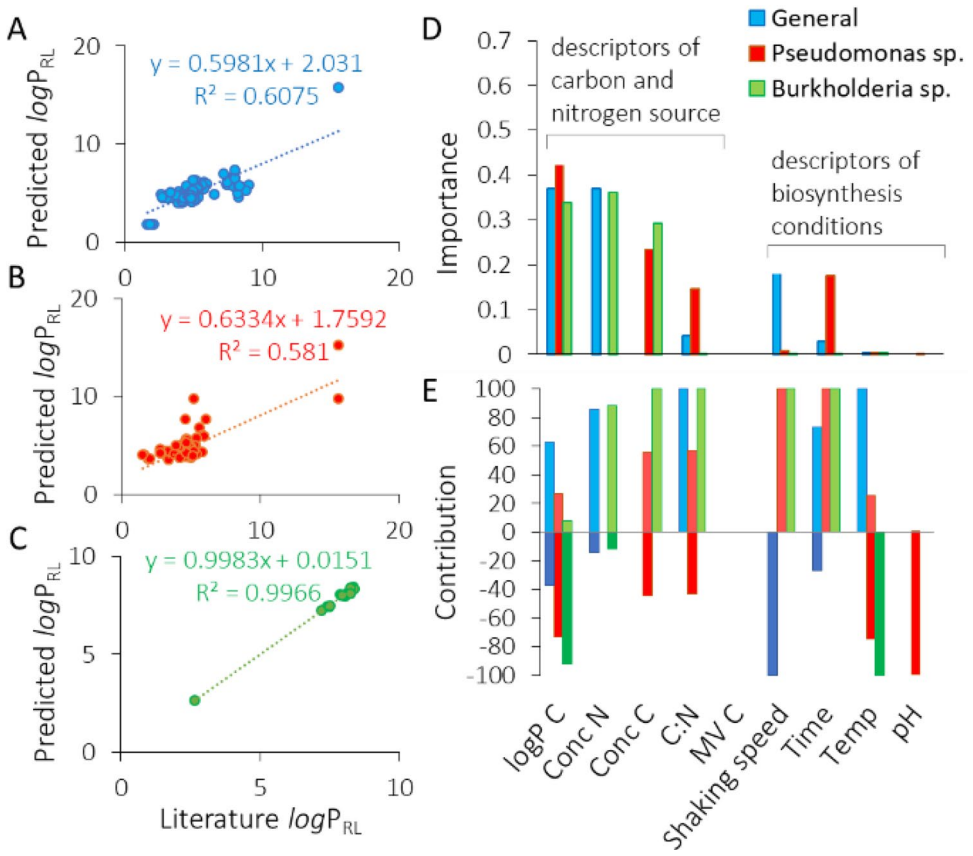

Figure 2. The estimated predictive power of the RL biosynthesis models: the general model for collated data (**A**) and separate models for Pseudomonas (**B**) or Burkholderia species (**C**). The importance of model variables (**D**) with respect to their positive or negative contribution to the predicted value (**E**). Model variables include descriptors of carbon and nitrogen sources as well as descriptors of environmental conditions of biosynthesis: *logPRL* and *logPC* logarithm of octanol–water partition coefficient for RL or carbon source, respectively, *Conc N* and *Conc C* concentration of nitrogen or carbon source, respectively, *C:N* carbon to nitrogen ratio, *MVC* the molecular volume of carbon source, *Temp* temperature.

($logP_C$) scoring the highest values among all the descriptors (importance of 0.37, 0.43 and 0.34 for the general, the *Pseudomonas* and the *Burkholderia* models, respectively). Both, the general and the *Burholderia* models showed high importance of nitrogen concentration (importance of 0.37 and 0.36, respectively). The concentration of carbon was the third most important descriptor, with an importance value of 0.23 for the *Pseudomonas* and 0.29 for the *Burkholderia* model. The C:N ratio was the fourth most important descriptor out of the group of carbon and nitrogen descriptors (importance of 0.04, 0.15 and 0.001 for the general, the *Pseudomonas* and the *Burkholderia* models, respectively) and fifth out of all examined descriptors in the general and the *Pseudomonas* models. In the general model, the C:N ratio was outperformed by the speed of shaking the culture (V, importance of 0.18) and the time of cultivation (importance of 0.17). Development of such models for predicting characteristics of the surface active products of biosynthesis is, to our best knowledge, presented for the first time. However, it is impossible to make a direct comparison of the obtained results with the literature. Most similar models that exist in the field of biosynthesis consider either enzymatic synthesis of cationic surfactant[138] or enzyme biosynthesis[139]. Masoumi et al.[138] have successfully predicted optimal conditions and enzyme amounts for enzymatic synthesis of triethanolamine based esterquat cationic surfactant. The model was characterized by a high coefficient of determination ($R^2_{\text{training set}} = 0.9079$, $R^2_{\text{test set}} = 0.9315$). Such a good fit is probably due to omitting the stage of microbial production, as the enzyme was applied. In turn, Banerjee and Bhattacharyya[139] have optimized the effect of inducers on protease biosynthesis by *Rhizopus oryzae*. Although the optimization resulted in a 2.5-fold increase in efficiency, the $R^2 = 0.0037$ (calculated from the data provided by the authors) of the model is definitely not a satisfying outcome.

An indirect comparison of the RL biosynthesis model with literature data can be based on the analysis of the effect of descriptors on the predicted parameter ($logP_{RL}$). When an increase in the numerical value of a descriptor leads to an increase in the value of a predicted parameter, a positive effect is credited to such a descriptor. Conversely, if a decrease in the value of a predicted parameter is observed, a negative effect is credited. And so, a positive effect of the hydrophobicity of carbon source ($logP_C$) was observed in 63% cases in the general RL biosynthesis model, 27% in the *Pseudomonas* model and only 8% in the *Burkholderia* model (Fig. 2E). The results obtained by Nicolo et al.[21] also presented positive effect. When they cultivated *Pseudomonas* on

low-*log*P-carbon-sources (*log*P_C of − 1.6 and − 2.64 for glycerol and glucose, respectively) preferentially low-*log*P-biosurfactant product was produced, i.e. BS dominated by diRL (*log*P_{RL} of 4.69 and 4.80 when growing on glycerol and glucose, respectively). In turn, when grown on high-*log*P-carbon-sources (*log*P_C of 6.05 and 10.84 for myristic acid and *brassica carrinata* oil, respectively), high-*log*P-biosurfactant product was obtained, where monoRL homologs were dominating (*log*P_{RL} of 4.88 and 5.15, respectively) (see SI, "RL production dataset"). A negative effect was observed *for Burkholderia glumae*[23], where cultivation on glycerol (*log*P_C, − 1.6) resulted in producing BS containing 98–99% diRL (*log*P_{RL} 7.95–8.04), whereas 88–96% of diRL (*log*P_{RL}, 7.20–7.52) was obtained when using rapeseed oil (*log*P_C 10.72) (see SI, "RL production dataset").

The effect of the second most important descriptor for the two models, the concentration of nitrogen, was mostly positive (in 85% and 88% cases in the general and the *Burkholderia* models, respectively, Fig. 2E). A vague positive effect was observed by Mata-Sandoval et al.[140] during the cultivation of *Pseudomonas* UG2 on corn oil and using $(NH_4)_2SO_4$ as a nitrogen source. The authors found that adding nutrients at once (higher starting concentration of nitrogen) resulted in a significant decrease in the share of diRL in the BS mixture (an increase of *log*P_{RL}) compared to adding nitrogen in six fractions at two-day intervals.

The third important descriptor, the concentration of carbon, had a rather positive or even exclusively positive effect on the RL hydrophobicity (55% and 100% cases in the *Pseudomonas* and the *Burkholderia* model, respectively, Fig. 2E). This suggests that increasing the concentration of carbon favors production of monoRL. The C:N ratio revealed mostly or exclusively positive contribution (100, 57 and 100% in the general, the *Pseudomonas* and the *Burkholderia* models, respectively). The descriptors of the biosynthesis conditions were mostly of a statistically insignificant importance to the models, except for the speed of shaking the culture in the general model and the time of cultivation in the *Pseudomonas* model (Fig. 2D). The contribution of the first one was 100% negative, whereas the contribution of the second one—100% positive (Fig. 2E). Nitschke et al.[49] and de Santana-Filho et al.[24] have found a negative influence of the time of cultivation on the hydrophobicity of RL produced by *Pseudomonas aeruginosa* LBI and *Pseudomonas aeruginosa* UFPEDA 614, respectively. They have stated that monoRLs are produced first, and with time they are transformed into diRLs. A negative effect of time was also observed for *Burkholderia glumae* AU6217 by Costa et al.[23] when grown on glycerol. But when grown on rapeseed oil, the effect was positive (SI, "RL Production Dataset).

Solubilization of triglycerides

Two TG species were chosen as solubilizates for experiments, namely tributyrin (TB) and triolein (TO). The MSR values estimated for the purpose of this study were in the range of 1.1×10^{-5} for TO solubilized in diRL solutions to 3×10^{-3} for TO solubilized in alkaline monoRL solutions, and were, in general, considerably lower than 90% of the collected literature MSR values (those ranged from 3×10^{-3} [134] for phenanthrene in RL solution to 7.44[124] for naphthalene in RL mixture) (SI, "MSR dataset").

MonoRL

The efficiency of TB solubilization in monoRL solutions decreased with increasing pH, with the average MSR_{TB} of 3.1×10^{-4} at pH 5.5 and only 5×10^{-5} at pH 8.5 (Fig. 3A). This is in accordance with previous observations

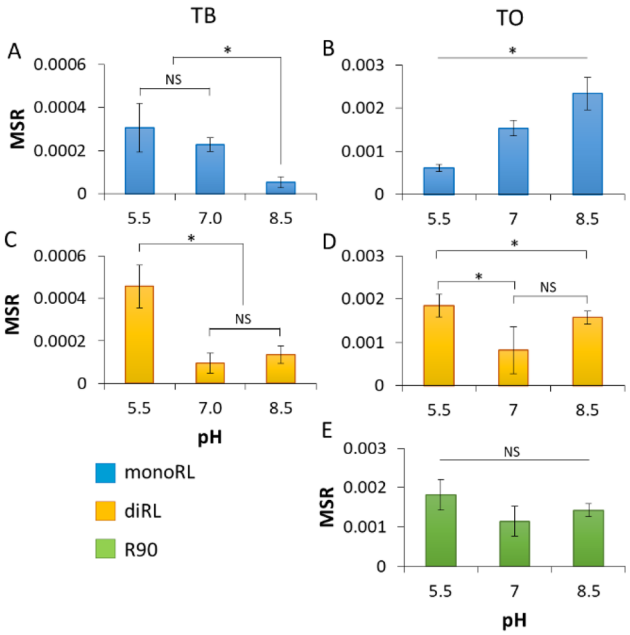

Figure 3. Influence of pH on the efficiency of micellar solubilization, expressed as molar solubilization ratio (MSR) for TB (**A**, **C**) and TO (**B**, **D**, **E**) in solutions of monoRL (**A**, **B**), diRL (**C**, **D**) or their mixture (R90) (**E**). *P < 0.05, by ANOVA; NS, P > 0.05, by ANOVA.

of Dahrazma et al.[141] and Eismin et al.[5] who stated that when increasing the pH, the structure of RL aggregates change from large to small vesicles and further to micelles, followed by a significant decrease of solubilizing capacity. However, the increase of MSR observed for TO upon increasing pH (Fig. 3B) is in contradiction with that statement. It suggests that the solubilization capacity is not solely a function of the surfactant aggregate type, but also the geometry of the surfactant and solubilizate molecules. Thus, the smaller and more hydrophilic TB (MV 297.46 $Å^3$, *log*P 3.27) probably is located in the core and palisade layer of aggregates, similarly as observed by Lin et al.[142] for solubilization of TB in diheptanoylphosphatidylcholine micelles[142]. In turn, hydrophobic and much bigger TO (*log*P 10.78, MV 984.58 $Å^3$) locates rather alongside monoRL molecules. We speculate that the double bond-dependent flexibility of the TO hydrophobic tails allows for fitting easily between RL molecules—an arrangement similar to how TO molecules locate themselves in mixed bilayers with phosphatidylcholine (PC)[143]. A previous ^{13}C NMR study showed that TO is located between PC molecules with carbonyl groups exposed to bulk solution. A similar molecular structure of PC and RL (i.e. both are double-tailed surfactants), as well as similar values of critical packing parameters (CPP of 0.62 for monoRL, 0.73 for diRL[144,145], and 0.60–0.61 for PC[146]) might suggest that TO located in the same manner in the RL systems examined here. Besides, the TO hydrocarbon tails are much longer (C18) than the hydrocarbon tails of TB (C4). Therefore, the entropic penalty to incorporate TO into a micelle is bigger. The hydrocarbon tails of TO are longer than those of RLs too (C7 hydrophobic moiety in β-hydroxydecanoic acid). Thus, when incorporated into a micelle, the TO molecules must fit between the surfactant molecules, therefore, pushing away one RL molecule from another and artificially extending the tail of the surfactant by several carbons[141]. Such extended tails form a new hydrophobic core of the micelle and consequently, the aggregate expands/swells. Distant RL molecules are more resistant to pH-induced micelle-rearrangement. Thus, in contrast to the solubilization of TB (Fig. 3A), we did not observe a decrease in the TO solubilization efficiency upon increasing the pH (Fig. 3B). Contrary to TO, TB does not have the ability to swell micelles[142].

As reported previously in the scientific literature, the pK_a values for RLs are in the range of 4.28 to 5.60[147,148]. Therefore, the higher the pH, the more dissociated RL is and the bigger the electrostatic repulsion between slightly acidic rhamnose head groups. Such repulsion virtually increases the size of the surfactant head and must rearrange the geometry of the micelle, where the created virtual spaces can be easily filled with TO molecules. This might explain the increase of MSRTO that we observed when increasing the pH (Fig. 3B). Opposite tendency has been observed by Luning Prak et al.[149], where the efficiency of solubilization was decreasing with an increase of the hydrocarbon chain length of the solubilizate. However, the solubilization in the aforementioned research was carried out for *n*-alkanes. Such hydrophobic molecules are incorporated in the hydrophobic core of the micelle, not in the palisade layer[150].

DiRL

Contrary to monoRL, the effect of pH on diRL solutions was less clear (Fig. 3 C,D). The highest average MSR values for both TB and TO were observed at a pH of 5.5 (4.6×10^{-4} and 1.8×10^{-3}, respectively). At this pH, RLs are either not dissociated or only slightly dissociated, as indicated by their low pK_a values (4.28 to 5.60[147,148]). Due to their rather nonionic behavior under these conditions, it is primarily the geometry that influences the packing of solubilizates into micelles. With two rhamnose moieties, diRL aggregates provide additional space in the palisade region. This allows for a greater quantity of both solubilizates to be incorporated compared to monoRL at pH 5.5 ($MSR_{TB} = 3.1 \times 10^{-4}$ and $MSR_{TO} = 6 \times 10^{-4}$, Fig. 3A,B). This observation aligns with the findings of Luning Prak et al.[149], which showed an increase in solubilization efficiency with the increase in polar heads of nonionic surfactants. Conversely, Zhang et al.[122] reported an opposite phenomenon, where the solubilization efficiency for phenanthrene was higher in monoRL than in diRL solutions, with MSRs of 5.7×10^{-2} and 2.1×10^{-2}, respectively. However, this could be attributed to the greater hydrophobicity of phenanthrene compared to the TG species examined in our research, resulting in a different solubilizate location within the micelle.

With an increase in pH to 7, we observed a significant decrease in average solubilization efficiency in diRL solutions, whereas an increase in pH to 8.5 resulted in enhanced average efficiency (Fig. 3C,D). This phenomenon may be attributed to the increasing repulsion forces between the large diRL headgroups, which consequently expands the palisade region space. In an alkaline environment, the small TB molecule fits into micelles even more effectively than in monoRL solutions, yielding a MSR value of 1.4×10^{-4} (Fig. 3C) as compared to 5×10^{-5} in monoRL solutions (Fig. 3A). However, this is not the case for TO, because it requires space not only in the palisade layer but also along the surfactant molecules. The repulsion, however, may not be sufficient for TO, as diRL is less ionic than monoRL even at a pH of 9, a behavior attributed to different intramolecular interactions and conformational changes[54]. This leads us to speculate that the solubilization capacity in diRL solutions is influenced more by geometric factors (overall size) and the resulting hydrophilicity (ratio of moieties) of BS molecules, rather than by electrostatic interactions. Therefore, the palisade layer of the micelle, under conditions favorable for TB and TO, shifts towards the core of the micelle due to the presence of a second rhamnose moiety. This shift results in a more pronounced decrease in TB solubilization, as TO locates along the BS molecules and causes micelle swelling, a phenomenon previously described for monoRLs (3.2.1. MonoRL). Consequently, the MSR values for solubilization of TO in diRL solutions were again higher (Fig. 3D) than those obtained for TB (Fig. 3C).

R90

The influence of pH on MSR values for TO solubilization in R90 (Fig. 3E), being the mixture of mono- and diRL, was more akin to that observed in diRL (Fig. 3D) than in monoRL solutions. Namely, the highest average MSR value was observed at pH 5.5, followed by pH 8.5 and 7. Considering it is monoRL that prevails R90 in mass (mono- and diRL 3:2 (w/w)), we can speculate that mixed micelle attributes are governed rather by bigger but

less ionic diRL. Further, the average MSR values for R90 measured at different pH did not differ significantly ($P > 0.05$, Fig. 3E), again underlying the similarity of R90 to diRL.

Summary

The obtained data indicate that the efficiency of solubilization results from both surfactant and solubilizate characteristics. Therefore, it seems reasonable to hypothesize that solubilization efficiency can be statistically predicted by modeling nonlinear dependencies on BS, solubilizate, and environmental descriptors. The experimental data on TGs solubilization were subsequently utilized to augment the database of solubilizates, allowing the model to encompass all potential applications of BS solutions in predicting the MSR. This new experimental data accounts for 23% of the entire dataset of MSR values compiled for this study (SI, "MSR dataset").

Modelling solubilizing potential of BS

Having expanded the MSR database with the newly obtained results on TGs solubilization, we developed a model to predict the influence of BS and solubilizate descriptors, as well as process conditions, on the efficiency of micellar solubilization. The MSR model demonstrates a good predictive power, with a coefficient of determination R^2 of 0.804 (Fig. 4A). Intriguingly, this model, which encompasses a broad spectrum of potential solubilizates, exhibits even greater predictive accuracy than our previous model (R^2 0.773)[8]. The latter was developed for a

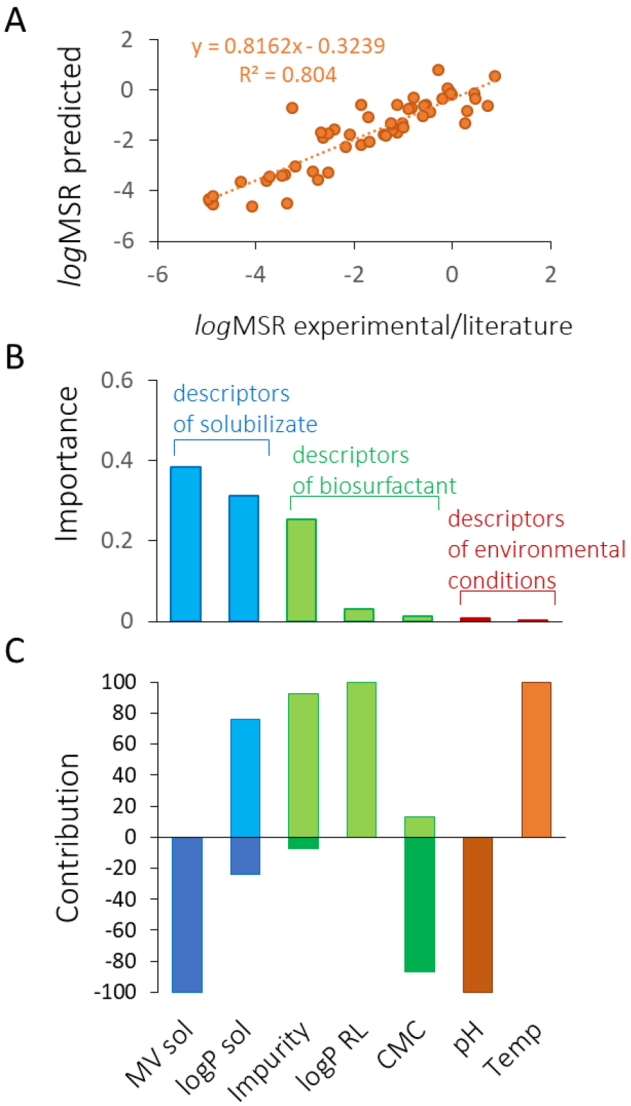

Figure 4. The estimated predictive power of the MSR model for calculating the solubilizing potential of BS, represented by logMSR (**A**), and the importance (**B**) and positive or negative contribution of various model variables (**C**). These variables encompass descriptors of the solubilizate, BS, and solubilization conditions, including MVsol (molecular volume of the solubilizate), *logPSOL* and *logPRL* logarithms of the octanol–water partition coefficients for solubilizate and *RL* respectively, *Impurity* based on a reversed BS purity scale[8,13], *CMC* critical micelle concentration, and *Temp* temperature.

much narrower range of solubilizates and specifically did not include data on TG species solubilization, as such data, to the best of our knowledge, were not previously available in the literature.

The analysis of the descriptors for their importance to the model clearly revealed that solubilizate characteristics are most crucial for efficient solubilization. The molecular volume of solubilizate (MV_{SOL}) showed the highest importance with a value of 0.384, followed by $logP_{SOL}$ with 0.312 (Fig. 4B). The third most important was the Impurity of BS, at the importance of 0.252. In comparison, the overall group of BS descriptors had lesser importance, with 0.031 and 0.013 for $logP_{RL}$ and CMC, respectively. This ranking places BS descriptors after those of the solubilizate. Environmental conditions, such as pH and temperature, were the least important in the MSR model, with respective importances of 0.0083 and 0.0002.

These findings align with our experimental results, where solubilizate characteristics (i.e., geometry and hydrophilicity) significantly influenced micellar solubilization in both mono- and diRL solutions. In contrast, pH showed a clear influence and trend only in the case of monoRL (Fig. 4). Notably, for the bioMSRcalc model[8], environmental conditions were more influential, followed by BS descriptors and solubilizate descriptors. This variation suggests that including MSR data for the solubilization of TG species is vital not only for the model's predictive power but also for accurately determining the importance of descriptors. The differences in hydrophobicity (*log*P of 3.27 and 10.78 for TB and TO, respectively) and molecular volume (MV of 297.46 and 984.58 $Å^3$ for TB and TO, respectively) of the TG species used in our experiments are substantial. These characteristics could notably expand the applicability domain of the model[151], as shown in Fig. 5A.

The MV of solubilizate exhibited a completely negative influence on the *log*MSR (100%, Fig. 4C). This is logical, considering that larger molecules are more challenging to incorporate into micelles. In turn, the hydrophobicity of the solubilizate ($logP_{SOL}$) showed a predominantly positive contribution (76%), indicating that the more hydrophobic the solubilizate, the higher the MSR. Concerning the impurity of BS, which is another significant descriptor (importance of 0.252, Fig. 4B), it also demonstrated a mainly positive effect (93%, Fig. 4C). This can be explained by the concept of competitive solubilization[152]. When impurities from insufficiently purified BS preparations compete for the same space in the micelle as the solubilizate does, they occupy areas typically reserved for the solubilizate, thus potentially reducing solubilization efficiency. Conversely, if the impurities occupy different locations within the micelle, this can lead to micellar swelling, thereby creating more space for the solubilizate and enhancing solubilization efficiency. According to the MSR model, impurities accompanying RL tend to cause micellar swelling, thereby increasing the efficiency of micellar solubilization.

Applicability domain of the models

Quantitative-Structure–Property Relationships (QSPR) are recommended by the European Community (e.g., REACH Article 1[153]) to aid in identifying the activity or properties of chemicals. However, these models are

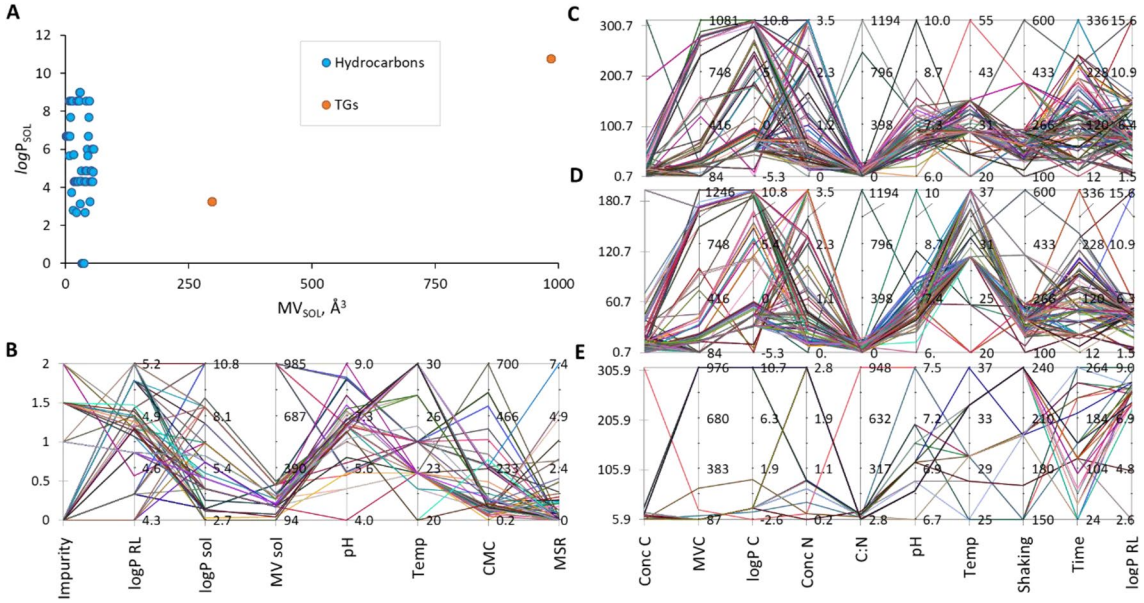

Figure 5. Comparative analysis of solubilizate descriptors for hydrocarbons and TGs, illustrating their respective potential to broaden the applicability domain of the model (**A**). Applicability domains for the MSR model (**B**), RL biosynthesis model (**C**), Pseudomonas model (**D**) and Burkholderia model (**E**) are presented in the form of parallel coordinates. Y-axis of applicability domains represents absolute values of the model descriptors: *Impurity* impurity of biosurfactant, *logPRL, logPsol* and *logPC* logarithm of octanol–water partition coefficient for RL, solubilizate or carbon source, *MVsol* and *MVC* molecular volume of solubilizate or carbon source in Å3; pH; *Temp* temperature in °C; *CMC* critical micelle concentration of RL in mg/L; *MSR* molar solubilization ratio, *ConcC* and *ConcN* concentration of carbon or nitrogen in mg/L, *C:N* carbon-to-nitrogen ratio; *Shaking* speed of shaking microbiological culture in rpm; *Time* time of biosynthesis in h. Each colored line represents one observation.

not without limitations. Primarily, the availability of experimental data in published works is constrained, and comparing results across different laboratories is challenging due to varying assumptions and methodologies. This heterogeneity leads to fragmented datasets and restricts the selection of model descriptors to those most commonly reported in the literature. Moreover, like all QSPR models, their accuracy is confined within their applicability domain—that is, the range of descriptor values on which the model was trained. Extrapolating results beyond this domain can introduce errors[151]. The applicability domains for the MSR model, the RL biosynthesis model, and the models for *Pseudomonas* and *Burkholderia* are illustrated in Fig. 5B–E. For instance, the MSR model applies to solubilizates with *log*P values between 2.7 and 10.6 and molecular volumes (MV) from 94 to 985 $Å^3$ (Fig. 5B). Detailed numeric descriptions of each model's applicability domain are provided in the supplementary information (SI—Equations, Tab.1).

Conclusions

In this study, we have combined three novel scientific endeavors. We conducted experimental investigations to describe the micellar solubilization of TG species in BS solutions. Additionally, we compiled databases from both literature and experimental sources concerning RL production during biosynthesis and RL application in the solubilization of various solubilizates. Utilizing these databases, we developed mathematical models that predict I. the composition of biosynthesized RLs based on biosynthesis parameters, and II. the efficiency of micellar solubilization considering the characteristics of RLs, the solubilizate, and the environmental conditions.

Our findings demonstrate that the characteristics of RLs, indicated by $logP_{RL}$, can be successfully predicted from the descriptors of carbon and nitrogen sources, and the conditions of microbial species cultivation. Among the three RL production models, the *Burkholderia* sp. model showed the highest coefficient of determination, followed by the general and the *Pseudomonas* sp. models.

In all three models, descriptors of carbon and nitrogen sources emerged as the most significant factors influencing the composition of the produced RLs. Notably, the hydrophobicity of the carbon source ($logP_C$) was identified as the most crucial parameter across the models. However, the influence of $logP_C$ on the characteristics of the produced BSs varied between the models.

The efficiency of micellar solubilization in RL solutions exhibited variations across different solubilizates, RL congeners, and pH conditions. We observed a distinct trend of pH influence, specifically in solubilizations using monoRL, which was not observed for diRL. Interestingly, the solubilization efficiency in R90 was more akin to that in diRL, despite monoRL being predominant in its composition.

By integrating our new experimental data with previous research[8] and a critical review of the latest literature, we have shown that the three most influential descriptors—MV and *log*P of solubilizate, as well as BS impurity—all had substantial effects on solubilization efficiency.

These models offer insights into how to cultivate microorganisms to produce BSs with specific solubilization properties. They can serve as computational guides in selecting the most suitable BS for solubilizing a desired substance in a formulation. For instance, in the context of environmentally friendly removal of contaminants from surfaces, one could first calculate the desired *log*P of a BS, providing required MSR range using the MSR calculator (SI, MSR calculator) along with possible environmental conditions. In the next step, using calculated $logP_{BS}$, one could determine cultivation conditions required to produce the requested BS (SI, RL production calculator).

To the best of our knowledge, this approach represents the first comprehensive methodology for developing RL-BS tailored to specific solubilization needs.

Data availability

All data generated or analysed during this study are included in this published article (and its Supplementary Information files).

Received: 18 December 2023; Accepted: 5 April 2024
Published online: 10 April 2024

References

1. Özdemir, G. & Sezgin, Ö. Keratin–rhamnolipids and keratin–sodium dodecyl sulfate interactions at the air/water interface. *Colloids Surf. B Biointerfaces* **52**(1), 1–7 (2006).
2. L.-K. Ju, S. Dashtbozorg, N. Vongpanish, Wound dressings with enhanced gas permeation and other beneficial properties, Google Patents, (2016).
3. Kłosowska-Chomiczewska, I. E., Medrzycka, K. & Karpenko, E. Biosurfactants—biodegradability, toxicity, efficiency in comparison with synthetic surfactants, In *Research and Application of New Technologies in Wastewater Treatment and Municipal Solid Waste Disposal in Ukraine, Sweden, and Poland, KTH/LWR/REPORT, Cracow, Poland*, (eds. P.E. Levlin E.) 1–9 (2011).
4. Li, G. *et al.* Evaluation of biodegradability and biotoxicity of surfactants in soil. *RSC Adv.* **7**(49), 31018–31026 (2017).
5. Eismin, R. J. *et al.* Evolution of aggregate structure in solutions of anionic monorhamnolipids: Experimental and computational results. *Langmuir* **33**(30), 7412–7424 (2017).
6. Rongsayamanont, W. *et al.* Formulation of crude oil spill dispersants based on the HLD concept and using a lipopeptide biosurfactant. *J. Hazard. Mater.* **334**, 168–177 (2017).
7. Resende, A. H. M. *et al.* Application of biosurfactants and chitosan in toothpaste formulation. *Colloids Surf. B Biointerfaces* **181**, 77 (2019).
8. Kłosowska-Chomiczewska, I. E. *et al.* Towards rational biosurfactant design—Predicting solubilization in rhamnolipid solutions. *Molecules* **26**(3), 534 (2021).
9. Al-Bahry, S. *et al.* Biosurfactant production by Bacillus subtilis B20 using date molasses and its possible application in enhanced oil recovery. *Int. Biodeterior. Biodegrad.* **81**, 141–146 (2013).
10. Luna, JMd., Sarubbo, L. & Campos-Takaki, GMd. A new biosurfactant produced by *Candida glabrata* UCP 1002: Characteristics of stability and application in oil recovery. *Braz. Arch. Biol. Technol.* **52**(4), 785–793 (2009).

11. Thavasi, R., Jayalakshmi, S. & Banat, I. M. Application of biosurfactant produced from peanut oil cake by *Lactobacillus delbrueckii* in biodegradation of crude oil. *Bioresour. Technol.* **102**(3), 3366–3372 (2011).
12. Luna, J. M., Rufino, R. D., Sarubbo, L. A. & Campos-Takaki, G. M. Characterisation, surface properties and biological activity of a biosurfactant produced from industrial waste by *Candida sphaerica* UCP0995 for application in the petroleum industry. *Colloids Surf. B Biointerfaces* **102**, 202–209 (2013).
13. Kłosowska-Chomiczewska, I. E. *et al.* Rhamnolipid CMC prediction. *J. Colloid Interface Sci.* **488**, 10–19 (2017).
14. Onwosi, C. O. & Odibo, F. J. C. Effects of carbon and nitrogen sources on rhamnolipid biosurfactant production by *Pseudomonas nitroreducens* isolated from soil. *World J. Microbiol. Biotechnol.* **28**(3), 937–942 (2012).
15. Santos, A. S. *et al.* Evaluation of different carbon and nitrogen sources in production of rhamnolipids by a strain of *Pseudomonas aeruginosa*. In *Biotechnology for Fuels and Chemicals* (eds Finkelstein, M. *et al.*) 1025–1035 (Springer, 2002).
16. Abouseoud, M., Maachi, R., Amrane, A., Boudergua, S. & Nabi, A. Evaluation of different carbon and nitrogen sources in production of biosurfactant by *Pseudomonas fluorescens*. *Desalination* **223**(1–3), 143–151 (2008).
17. Hošková, M. *et al.* Characterization of rhamnolipids produced by non-pathogenic *Acinetobacter* and *Enterobacter* bacteria. *Bioresour. Technol.* **130**, 510–516 (2013).
18. Mehdi, S., Dondapati, J. S. & Rahman, P. Influence of nitrogen and phosphorus on rhamnolipid biosurfactant production by *Pseudomonas aeruginosa* DS10-129 using glycerol as carbon source. *Biotechnology* **10**(2), 183–189 (2011).
19. Varjani, S. J. & Upasani, V. N. Carbon spectrum utilization by an indigenous strain of *Pseudomonas aeruginosa* NCIM 5514: Production, characterization and surface active properties of biosurfactant. *Bioresour. Technol.* **221**, 510–516 (2016).
20. Nitschke, M. *et al.* Oil wastes as unconventional substrates for rhamnolipid biosurfactant production by *Pseudomonas aeruginosa* LBI. *Biotechnol. Prog.* **21**(5), 1562–1566 (2005).
21. Nicolò, M. S. *et al.* Carbon source effects on the mono/dirhamnolipid ratio produced by *Pseudomonas aeruginosa* L05, a new human respiratory isolate. *New biotechnol.* **39**, 36–41 (2017).
22. dos Santos, A. S., Pereira, N. Jr. & Freire, D. M. Strategies for improved rhamnolipid production by *Pseudomonas aeruginosa* PA1. *PeerJ* **4**, e2078 (2016).
23. Costa, S., Déziel, E. & Lépine, F. Characterization of rhamnolipid production by *Burkholderia glumae*. *Lett. Appl. Microbial.* **53**(6), 620–627 (2011).
24. de Santana-Filho, A. P. *et al.* Evaluation of the structural composition and surface properties of rhamnolipid mixtures produced by *Pseudomonas aeruginosa* UFPEDA 614 in different cultivation periods. *Appl. Biochem. Biotechnol.* **175**(2), 988–995 (2015).
25. Ismail, W. *et al.* Stimulation of rhamnolipid biosurfactants production in *Pseudomonas aeruginosa* AK6U by organosulfur compounds provided as sulfur sources. *Biotechnol. Rep.* **7**, 55–63 (2015).
26. Abalos, A., Maximo, F., Manresa, M. A. & Bastida, J. Utilization of response surface methodology to optimize the culture media for the production of rhamnolipids by *Pseudomonas aeruginosa* AT10. *J. Chem. Technol. Biotechnol. Int. Res. Process Environ. Clean Technol.* **77**(7), 777–784 (2002).
27. Hassan, M., Essam, T., Yassin, A. S. & Salama, A. Optimization of rhamnolipid production by biodegrading bacterial isolates using Plackett-Burman design. *Int. J. Boil. Macromol* **82**, 573–579 (2016).
28. Onwosi, C. & Odibo, F. Use of response surface design in the optimization of starter cultures for enhanced rhamnolipid production by *Pseudomonas nitroreducens*. *Afr. J. Biotechnol.* **12**(19), 2611–2617 (2013).
29. Chen, I.-C. & Lee, M.-T. Rhamnolipid biosurfactants for oil recovery: Salt effects on the structural properties investigated by mesoscale simulations. *ACS omega* **7**(7), 6223–6237 (2022).
30. Posada-Baquero, R., Grifoll, M. & Ortega-Calvo, J.-J. Rhamnolipid-enhanced solubilization and biodegradation of PAHs in soils after conventional bioremediation. *Sci. Total Environ.* **668**, 790–796 (2019).
31. Liu, C. *et al.* Response surface methodology for the optimization of the ultrasonic-assisted rhamnolipid treatment of oily sludge. *Arab. J. Chem.* **14**(3), 102971 (2021).
32. Liu, C. *et al.* Optimization of process parameters of rhamnolipid treatment of oily sludge based on response surface methodology. *ACS omega* **5**(45), 29333–29341 (2020).
33. Gholami, A. & Khoshdast, H. Using artificial neural networks for the intelligent estimation of selectivity index and metallurgical responses of a sample coal bioflotation by rhamnolipid biosurfactants. *Energy Sources A Recovery Utili. Environ. Eff.* https://doi.org/10.1080/15567036.2020.1857477 (2020).
34. Chen, F., Huang, J., Wu, X., Wu, X. & Arabmarkadeh, A. On the evaluation of rhamnolipid biosurfactant adsorption performance on amberlite XAD-2 using machine learning techniques. *BioMed Res. Int.* **2021**(1), 10 (2021).
35. Sim, L., Ward, O. & Li, Z. Production and characterisation of a biosurfactant isolated from *Pseudomonas aeruginosa* UW-1. *J. Ind. Microbiol. Biotechnol.* **19**(4), 232–238 (1997).
36. Pereira, J. F. *et al.* Characterization by electrospray ionization and tandem mass spectrometry of rhamnolipids produced by two *Pseudomonas aeruginosa* strains isolated from Brazilian crude oil. *Eur. J. Mass Spectrom.* **18**(4), 399–406 (2012).
37. Pennell, K. D., Adinolfi, A. M., Abriola, L. M. & Diallo, M. S. Solubilization of dodecane, tetrachloroethylene, and 1, 2-dichlorobenzene in micellar solutions of ethoxylated nonionic surfactants. *Environ. Sci. Technol.* **31**(5), 1382–1389 (1997).
38. Aryal, M. Performance and potential of bacterial biodegradation of polycyclic aromatic hydrocarbons from micellar solutions. *Environ. Technol. Rev.* **10**(1), 342–365 (2021).
39. J. Brophy, D. Bawden, Is Google enough? Comparison of an internet search engine with academic library resources, Aslib Proc. 57(6) 498-512. (2005).
40. Lovaglio, R., Silva, V., Ferreira, H., Hausmann, R. & Contiero, J. Rhamnolipids know-how: looking for strategies for its industrial dissemination. *Biotechnol. Adv.* **33**(8), 1715–1726 (2015).
41. Lopes, P. R. M. *et al.* Production of rhamnolipids from soybean soapstock: Characterization and comparation with synthetics surfactants. *Waste Biomass Valoriz.* **12**(4), 2013–2023 (2021).
42. Thio, C. W., Lim, W. H., Shah, U. KMd. & Phang, L.-Y. Palm kernel fatty acid distillate as substrate for rhamnolipids production using *Pseudomonas* sp. LM19. *Green Chem. Lett. Rev.* **15**(1), 81–92 (2022).
43. Mata-Sandoval, J. C., Karns, J. & Torrents, A. High-performance liquid chromatography method for the characterization of rhamnolipid mixtures produced by *Pseudomonas aeruginosa* UG2 on corn oil. *J. Chromatogr. A* **864**(2), 211–220 (1999).
44. Jadhav, J., Dutta, S., Kale, S. & Pratap, A. Fermentative production of rhamnolipid and purification by adsorption chromatography. *Prep. Biochem. Biotechnol.* **48**(3), 234–241 (2018).
45. Zhou, J. *et al.* High di-rhamnolipid production using *Pseudomonas aeruginosa* KT1115, separation of mono/di-rhamnolipids, and evaluation of their properties. *Front. Bioeng. Biotechnol.* https://doi.org/10.3389/fbioe.2019.00245 (2019).
46. Gong, Z., Peng, Y. & Wang, Q. Rhamnolipid production, characterization and fermentation scale-up by *Pseudomonas aeruginosa* with plant oils. *Biotechnol. Lett.* **37**(10), 2033–2038 (2015).
47. Wang, Q. *et al.* Engineering bacteria for production of rhamnolipid as an agent for enhanced oil recovery. *Biotechnol. Bioeng.* **98**(4), 842–853 (2007).
48. Arutchelvi, J. & Doble, M. Characterization of glycolipid biosurfactant from *Pseudomonas aeruginosa* CPCL isolated from petroleum-contaminated soil. *Lett. Appl. Microbial.* **51**(1), 75–82 (2010).
49. Nitschke, M., Costa, S. G. & Contiero, J. Structure and applications of a rhamnolipid surfactant produced in soybean oil waste. *Appl. Biochem. Biotechnol.* **160**(7), 2066–2074 (2010).

50. Monteiro, S. A. *et al.* Molecular and structural characterization of the biosurfactant produced by *Pseudomonas aeruginosa* DAUPE 614. *Chem. Phys. Lipids* **147**(1), 1–13 (2007).
51. Abdel-Mawgoud, A. M., Aboulwafa, M. M. & Hassouna, N.A.-H. Characterization of rhamnolipid produced by *Pseudomonas aeruginosa* isolate Bs20. *Appl. Biochem. Biotechnol.* **157**(2), 329–345 (2009).
52. Costa, S. G. *et al.* Cassava wastewater as a substrate for the simultaneous production of rhamnolipids and polyhydroxyalkanoates by *Pseudomonas aeruginosa*. *J. Ind. Microbiol. Biotechnol.* **36**(8), 1063–1072 (2009).
53. Dubeau, D., Déziel, E., Woods, D. E. & Lépine, F. *Burkholderia thailandensis* harbors two identical rhl gene clusters responsible for the biosynthesis of rhamnolipids. *BMC Microbial.* **9**(1), 1–12 (2009).
54. Guo, Y.-P., Hu, Y.-Y., Gu, R. R. & Lin, H. Characterization and micellization of rhamnolipidic fractions and crude extracts produced by *Pseudomonas aeruginosa* mutant MIG-N146. *J. Colloid Interface Sci.* **331**(2), 356–363 (2009).
55. Rooney, A. P., Price, N. P., Ray, K. J. & Kuo, T.-M. Isolation and characterization of rhamnolipid-producing bacterial strains from a biodiesel facility. *FEMS Microbial. Lett.* **295**(1), 82–87 (2009).
56. Yin, H. *et al.* Characteristics of biosurfactant produced by *Pseudomonas aeruginosa* S6 isolated from oil-containing wastewater. *Process Biochem.* **44**(3), 302–308 (2009).
57. Christova, N. *et al.* Chemical characterization and physical and biological activities of rhamnolipids produced by *Pseudomonas aeruginosa* BN10. *Zeitschrift für Naturforschung C* **66**(7–8), 394–402 (2011).
58. Górna, H., Ławniczak, Ł, Zgoła-Grześkowiak, A. & Kaczorek, E. Differences and dynamic changes in the cell surface properties of three *Pseudomonas aeruginosa* strains isolated from petroleum-polluted soil as a response to various carbon sources and the external addition of rhamnolipids. *Bioresour. Technol.* **102**(3), 3028–3033 (2011).
59. Morris, J. D. *et al.* Imaging and analysis of *Pseudomonas aeruginosa* swarming and rhamnolipid production. *Appl. Environ. Microbial.* **77**(23), 8310–8317 (2011).
60. Müller, M. M., Hörmann, B., Kugel, M., Syldatk, C. & Hausmann, R. Evaluation of rhamnolipid production capacity of *Pseudomonas aeruginosa* PAO1 in comparison to the rhamnolipid over-producer strains DSM 7108 and DSM 2874. *Appl. Microbial. Biotechnol.* **89**(3), 585–592 (2011).
61. Pratap, A., Wadekar, S., Kale, S., Lali, A. & Bhowmick, D. N. Non-traditional oils as newer feedstock for rhamnolipids production by *Pseudomonas aeruginosa* (ATCC 10145). *J. Am. Oil Chem. Soc.* **88**(12), 1935–1943 (2011).
62. Wadekar, S. *et al.* Structural elucidation and surfactant properties of rhamnolipids synthesized by *Pseudomonas aeruginosa* (ATCC 10145) on sweet water as carbon source and stabilization effect on foam produced by sodium lauryl sulfate. *Tenside Surfactants Deterg.* **48**(4), 286–292 (2011).
63. Wadekar, S. *et al.* Study of glycerol residue as a carbon source for production of rhamnolipids by *Pseudomonas aeruginosa* (ATCC 10145). *Tenside Surfactants Deterg.* **48**(1), 16–22 (2011).
64. Worakitsiri, P. *et al.* Synthesis of polyaniline nanofibers and nanotubes via rhamnolipid biosurfactant templating. *Synth. Metals* **161**(3–4), 298–306 (2011).
65. Rikalović, M., Gojgić-Cvijović, G., Vrvić, M. & Karadžić, I. Production and characterization of rhamnolipids from *Pseudomonas aeruginosa* san-ai. *J. Serb. Chem. Soc.* **77**(1), 27–42 (2012).
66. Samadi, N. *et al.* Structural characterization and surface activities of biogenic rhamnolipid surfactants from *Pseudomonas aeruginosa* isolate MN1 and synergistic effects against methicillin-resistant *Staphylococcus aureus*. *Folia microbial.* **57**(6), 501–508 (2012).
67. Zhang, L., Veres-Schalnat, T. A., Somogyi, A., Pemberton, J. E. & Maier, R. M. Fatty acid cosubstrates provide β-oxidation precursors for rhamnolipid biosynthesis in *Pseudomonas aeruginosa*, as evidenced by isotope tracing and gene expression assays. *Appl. Environ. Microbial.* **78**(24), 8611–8622 (2012).
68. Nalini, S. & Parthasarathi, R. Biosurfactant production by *Serratia rubidaea* SNAU02 isolated from hydrocarbon contaminated soil and its physico-chemical characterization. *Bioresour. Technol.* **147**, 619–622 (2013).
69. Pereira, A. G. *et al.* Optimization of biosurfactant production using waste from biodiesel industry in a new membrane assisted bioreactor. *Process Biochem.* **48**(9), 1271–1278 (2013).
70. Rikalovic, M. G. *et al.* Comparative analysis of rhamnolipids from novel environmental isolates of *Pseudomonas aeruginosa*. *J. Surfactants Deterg.* **16**(5), 673–682 (2013).
71. Singh, A. K. & Cameotra, S. S. Rhamnolipids production by multi-metal-resistant and plant-growth-promoting rhizobacteria. *Appl. Biochem. Biotechnol.* **170**(5), 1038–1056 (2013).
72. Tavares, L. F. *et al.* Characterization of rhamnolipids produced by wild-type and engineered *Burkholderia kururiensis*. *Appl. Microbial. Biotechnol.* **97**, 1909–1921 (2013).
73. Liu, J.-F., Wu, G., Yang, S.-Z. & Mu, B.-Z. Structural characterization of rhamnolipid produced by *Pseudonomas aeruginosa* strain FIN2 isolated from oil reservoir water. *World J. Microbiol. Biotechnol.* **30**(5), 1473–1484 (2014).
74. Haba, E., Pinazo, A., Pons, R., Pérez, L. & Manresa, A. Complex rhamnolipid mixture characterization and its influence on DPPC bilayer organization. *Biochim. Biophys. Acta* **1838**, 776 (2014).
75. Han, L. *et al.* Engineering the biosynthesis of novel rhamnolipids in *E scherichia* coli for enhanced oil recovery. *J. Appl. Microbial.* **117**(1), 139–150 (2014).
76. Zhang, L., Pemberton, J. E. & Maier, R. M. Effect of fatty acid substrate chain length on *Pseudomonas aeruginosa* ATCC 9027 monorhamnolipid yield and congener distribution. *Process Biochem.* **49**(6), 989–995 (2014).
77. Hošková, M. *et al.* Structural and physiochemical characterization of rhamnolipids produced by *Acinetobacter calcoaceticus*, *Enterobacter asburiae* and *Pseudomonas aeruginosa* in single strain and mixed cultures. *J. Biotechnol.* **193**, 45–51 (2015).
78. Behrens, B., Engelen, J., Tiso, T., Blank, L. M. & Hayen, H. Characterization of rhamnolipids by liquid chromatography/mass spectrometry after solid-phase extraction. *Anal. Bioanal. Chem.* **408**(10), 2505–2514 (2016).
79. Yela, A. C. A. *et al.* A comparison between conventional *Pseudomonas aeruginosa* rhamnolipids and *Escherichia* coli transmembrane proteins for oil recovery enhancing. *Int. Biodeterior. Biodegrad.* **112**, 59–65 (2016).
80. Reddy, K. S., Khan, M. Y., Archana, K., Reddy, M. G. & Hameeda, B. Utilization of mango kernel oil for the rhamnolipid production by *Pseudomonas aeruginosa* DR1 towards its application as biocontrol agent. *Bioresour. Technol.* **221**, 291–299 (2016).
81. Anic, I., Nath, A., Franco, P. & Wichmann, R. Foam adsorption as an ex situ capture step for surfactants produced by fermentation. *J. Biotechnol.* **258**, 181–189 (2017).
82. Elshikh, M. *et al.* Rhamnolipids from non-pathogenic *Burkholderia thailandensis* E264: Physicochemical characterization, antimicrobial and antibiofilm efficacy against oral hygiene related pathogens. *New Biotechnol.* **36**, 26–36 (2017).
83. Funston, S. J. *et al.* Enhanced rhamnolipid production in *Burkholderia thailandensis* transposon knockout strains deficient in polyhydroxyalkanoate (PHA) synthesis. *Appl. Microbial. Biotechnol* **101**(23), 8443–8454 (2017).
84. Cheng, T. *et al.* A novel rhamnolipid-producing *Pseudomonas aeruginosa* ZS1 isolate derived from petroleum sludge suitable for bioremediation. *AMB Express* **7**(1), 1–14 (2017).
85. Lotfabad, T. B., Ebadipour, N., Roostaazad, R., Partovi, M. & Bahmaei, M. Two schemes for production of biosurfactant from *Pseudomonas aeruginosa* MR01: Applying residues from soybean oil industry and silica sol–gel immobilized cells. *Colloids Surf. B Biointerfaces* **152**, 159–168 (2017).
86. Partovi, M., Lotfabad, T. B., Roostaazad, R., Bahmaei, M. & Tayyebi, S. Management of soybean oil refinery wastes through recycling them for producing biosurfactant using *Pseudomonas aeruginosa* MR01. *World J. Microbiol. Biotechnol.* **29**(6), 1039–1047 (2013).

87. Kourmentza, C. *et al. Burkholderia thailandensis* as a microbial cell factory for the bioconversion of used cooking oil to polyhydroxyalkanoates and rhamnolipids. *Bioresour. Technol.* **247**, 829–837 (2018).
88. Zhao, F., Shi, R., Ma, F., Han, S. & Zhang, Y. Oxygen effects on rhamnolipids production by *Pseudomonas aeruginosa*. *Microb. Cell Factor.* **17**, 3483 (2018).
89. Irorere, V. U. *et al.* Fatty acid synthesis pathway provides lipid precursors for rhamnolipid biosynthesis in *Burkholderia thailandensis* E264. *Appl. Microbial. Biotechnol.* **102**(14), 6163–6174 (2018).
90. Radzuan, M. N., Banat, I. M. & Winterburn, J. Biorefining palm oil agricultural refinery waste for added value rhamnolipid production via fermentation. *Ind. Crops Prod.* **116**, 64–72 (2018).
91. Sodagari, M., Invally, K. & Ju, L.-K. Maximize rhamnolipid production with low foaming and high yield. *Enzyme Microb. Technol.* **110**, 79–86 (2018).
92. Twigg, M. S. *et al.* Identification and characterisation of short chain rhamnolipid production in a previously uninvestigated, non-pathogenic marine pseudomonad. *Appl. Microbial. Biotechnol.* **102**(19), 8537–8549 (2018).
93. Bazsefidpar, S., Mokhtarani, B., Panahi, R. & Hajfarajollah, H. Overproduction of rhamnolipid by fed-batch cultivation of *Pseudomonas aeruginosa* in a lab-scale fermenter under tight DO control. *Biodegradation* **30**(1), 59–69 (2019).
94. Tripathi, L. *et al.* Biosynthesis of rhamnolipid by a *Marinobacter* species expands the paradigm of biosurfactant synthesis to a new genus of the marine microflora. *Microb. cell Factor.* **18**(1), 1–12 (2019).
95. Du, J., Zhang, A., Zhang, X., Si, X. & Cao, J. Comparative analysis of rhamnolipid congener synthesis in neotype *Pseudomonas aeruginosa* ATCC 10145 and two marine isolates. *Bioresour. Technol.* **286**, 121380 (2019).
96. Nurfarahin, A. H., Mohamed, M. S. & Phang, L. Y. Development of palm fatty acid distillate-containing medium for biosurfactant production by *Pseudomonas* sp. LM19. *Molecules* **24**(14), 2613 (2019).
97. Sharma, S., Datta, P., Kumar, B., Tiwari, P. & Pandey, L. M. Production of novel rhamnolipids via biodegradation of waste cooking oil using *Pseudomonas aeruginosa* MTCC7815. *Biodegradation* **30**(4), 301–312 (2019).
98. Zhao, F. *et al.* Production of rhamnolipids with different proportions of mono-rhamnolipids using crude glycerol and a comparison of their application potential for oil recovery from oily sludge. *RSC Adv.* **9**(6), 2885–2891 (2019).
99. Victor, I. U. *et al.* Quorum sensing as a potential target for increased production of rhamnolipid biosurfactant in *Burkholderia thailandensis* E264. *Appl. Microbial. Biotechnol.* **103**(16), 6505–6517 (2019).
100. Zhao, F., Han, S. & Zhang, Y. Comparative studies on the structural composition, surface/interface activity and application potential of rhamnolipids produced by *Pseudomonas aeruginosa* using hydrophobic or hydrophilic substrates. *Bioresour. Technol.* **295**, 122269 (2020).
101. Buonocore, C. *et al.* Characterization of a new mixture of mono-rhamnolipids produced by *Pseudomonas gessardii* isolated from Edmonson Point (Antarctica). *Mar. Drugs* **18**(5), 269 (2020).
102. Diab, A. M., Ibrahim, S. & Abdulla, H. M. Safe application and preservation efficacy of low-toxic rhamnolipids produced from *Ps aeruginosa* for cosmetics and personal care formulation. *Egypt. J. Microbiol.* **55**, 57–70 (2020).
103. Sen, S., Borah, S. N., Bora, A. & Deka, S. Rhamnolipid exhibits anti-biofilm activity against the dermatophytic fungi *Trichophyton rubrum* and *Trichophyton mentagrophytes*. *Biotechnol. Rep.* **27**, e00516 (2020).
104. Rocha, V. A. L. *et al.* Antibiofilm effect of mono-rhamnolipids and di-rhamnolipids on carbon steel submitted to oil produced water. *Biotechnol. Prog.* **37**(3), e3131 (2021).
105. Sun, H. *et al.* Optimization and characterization of rhamnolipid production by *Pseudomonas aeruginosa* NY3 using waste frying oil as the sole carbon. *Biotechnol. Prog.* **37**(4), e3155 (2021).
106. Radzuan, M. N., Winterburn, J. & Banat, I. Bioreactor rhamnolipid production using palm oil agricultural refinery by-products. *Processes* **9**(11), 2037 (2021).
107. Chebbi, A. *et al. Burkholderia thailandensis* E264 as a promising safe rhamnolipids' producer towards a sustainable valorization of grape marcs and olive mill pomace. *Appl. Microbial. biotechnol.* **105**, 3825–3842 (2021).
108. Rashid, N. F. M., Amelia, T. S. M., Amirul, A.-A.A. & Bhubalan, K. Dual-production of polyhydroxyalkanoate and rhamnolipid by *Pseudomonas aeruginosa* UMTKB-5 using industrial by-products, Malaysian. *J Anal Sci* **25**, 24–39 (2021).
109. Zhao, F., Yuan, M., Lei, L., Li, C. & Xu, X. Enhanced production of mono-rhamnolipid in *Pseudomonas aeruginosa* and application potential in agriculture and petroleum industry. *Bioresour. Technol.* **323**, 124605 (2021).
110. Ahmad, Z. *et al.* Production, functional stability, and effect of rhamnolipid biosurfactant from *Klebsiella* sp. on phenanthrene degradation in various medium systems. *Ecotoxicol. Environ. Saf.* **207**, 111514 (2021).
111. Zhu, P. *et al.* Rhamnolipids from non-pathogenic *Acinetobacter calcoaceticus*: Bioreactor-scale production, characterization and wound healing potency. *New Biotechnol.* **67**, 23–31 (2022).
112. Funston, S. J. *et al.* Characterising rhamnolipid production in *Burkholderia thailandensis* E264, a non-pathogenic producer. *Appl. Microbiol. Biotechnol.* **100**(18), 7945–7956 (2016).
113. Liu, Y. *et al.* Effect of rhamnolipid solubilization on hexadecane bioavailability: Enhancement or reduction?. *J. hazard. Mater.* **322**, 394–401 (2017).
114. Zhong, H. *et al.* Aggregate-based sub-CMC solubilization of n-alkanes by monorhamnolipid biosurfactant. *New J. Chem.* **40**(3), 2028–2035 (2016).
115. Wan, J. *et al.* Simultaneous removal of lindane, lead and cadmium from soils by rhamnolipids combined with citric acid. *PLoS One* **10**(6), e0129978 (2015).
116. Zhong, H. *et al.* Degradation of pseudo-solubilized and mass hexadecane by a *Pseudomonas aeruginosa* with treatment of rhamnolipid biosurfactant. *Int. Biodeterior. Biodegrad.* **94**, 152–159 (2014).
117. Guo, Y., Mulligan, C. N. & Nieh, M.-P. An unusual morphological transformation of rhamnolipid aggregates induced by concentration and addition of styrene: A small angle neutron scattering (SANS) study. *Colloids Surf. A Physicochem. Eng. Asp.* **373**(1–3), 42–50 (2011).
118. Wan, J., Chai, L., Lu, X., Lin, Y. & Zhang, S. Remediation of hexachlorobenzene contaminated soils by rhamnolipid enhanced soil washing coupled with activated carbon selective adsorption. *J. hazard. Mater.* **189**(1–2), 458–464 (2011).
119. Shin, K.-H., Kim, J.-Y. & Kim, K.-W. Effect of biosurfactant addition on the biodegradation of phenanthrene in soil-water system. *Environ. Eng. Res.* **13**(1), 8–13 (2008).
120. Clifford, J. S., Ioannidis, M. A. & Legge, R. L. Enhanced aqueous solubilization of tetrachloroethylene by a rhamnolipid biosurfactant. *J. Colloid Interface Sci.* **305**(2), 361–365 (2007).
121. Bai, G., Brusseau, M. L. & Miller, R. M. Influence of cation type, ionic strength, and pH on solubilization and mobilization of residual hydrocarbon by a biosurfactant. *J. Contam. Hydrol.* **30**(3–4), 265–279 (1998).
122. Zhang, Y., Maier, W. J. & Miller, R. M. Effect of rhamnolipids on the dissolution, bioavailability, and biodegradation of phenanthrene. *Environ. Sci. Technol.* **31**(8), 2211–2217 (1997).
123. Zhang, Y. & Miller, R. M. Effect of rhamnolipid (biosurfactant) structure on solubilization and biodegradation of n-alkanes. *Appl. Environ. Microbiol.* **61**(6), 2247–2251 (1995).
124. Li, S. *et al.* Effect of rhamnolipid biosurfactant on solubilization of polycyclic aromatic hydrocarbons. *Mar. Pollut. Bull.* **101**(1), 219–225 (2015).
125. Zhang, X., Guo, Q., Hu, Y. & Lin, H. Effects of monorhamnolipid and dirhamnolipid on sorption and desorption of triclosan in sediment–water system. *Chemosphere* **90**(2), 581–587 (2013).

126. Zhu, S., Liang, S. & You, X. Effect of rhamnolipid biosurfactant on solubilization and biodegradation of polycyclic aromatic hydrocarbons. In *2013 Third International Conference on Intelligent System Design and Engineering Applications* (eds Zhu, S. *et al.*) 651–654 (IEEE, 2013).
127. Harendra, S. & Vipulanandan, C. Degradation of high concentrations of PCE solubilized in SDS and biosurfactant with Fe/Ni bi-metallic particles. *Colloids Surf. A Physicochem. Eng. Asp.* **322**(1–3), 6–13 (2008).
128. Bordas, F., Lafrance, P. & Villemur, R. Conditions for effective removal of pyrene from an artificially contaminated soil using *Pseudomonas aeruginosa* 57SJ rhamnolipids. *Environ. Pollut.* **138**(1), 69–76 (2005).
129. Thangamani, S. & Shreve, G. S. Effect of anionic biosurfactant on hexadecane partitioning in multiphase systems. *Environ. Sci. Technol.* **28**(12), 1993–2000 (1994).
130. Zang, T., Wu, H., Yan, B., Zhang, Y. & Wei, C. Enhancement of PAHs biodegradation in biosurfactant/phenol system by increasing the bioavailability of PAHs. *Chemosphere* **266**, 128941 (2021).
131. Li, K., Yang, B. & Wang, L. Performance evaluation of a biotrickling filter for the removal of gas-phase 1, 2-dichlorobenzene: Influence of rhamnolipid and ferric ions. *Chemosphere* **250**, 126261 (2020).
132. Liu, J., Wang, Y. & Li, H. Synergistic solubilization of phenanthrene by mixed micelles composed of biosurfactants and a conventional non-ionic surfactant. *Molecules* **25**(18), 4327 (2020).
133. Li, Y. *et al.* Surface properties and solubility enhancement of Gemini/conventional surfactant mixtures based on sulfonate Gemini surfactant. *J. Mol. Liq.* **276**, 488–496 (2019).
134. Meng, L., Li, W., Bao, M. & Sun, P. Effect of surfactants on the solubilization, sorption and biodegradation of benzo (a) pyrene by *Pseudomonas aeruginosa* BT-1. *J. Taiwan Inst. Chem. Eng.* **96**, 121–130 (2019).
135. Sun, S. *et al.* A biosurfactant-producing *Pseudomonas aeruginosa* S5 isolated from coking wastewater and its application for bioremediation of polycyclic aromatic hydrocarbons. *Bioresour. Technol.* **281**, 421–428 (2019).
136. M. Chemoinformatics, Molinspiration, Brastislava, Slovak Republic, (2014).
137. Łozińska, N., Głowacz-Różyńska, A., Artichowicz, W., Lu, Y. & Jungnickel, C. Microencapsulation of fish oil–determination of optimal wall material and encapsulation methodology. *J. Food Eng.* **268**, 109730 (2020).
138. Masoumi, H. R. F., Kassim, A., Basri, M., Abdullah, D. K. & Haron, M. J. Multivariate optimization in the biosynthesis of a triethanolamine (TEA)-based esterquat cationic surfactant using an artificial neural network. *Molecules* **16**(7), 5538–5549 (2011).
139. Banerjee, R. & Bhattacharyya, B. Optimization of multiple inducers effect on protease biosynthesis by *Rhizopus oryzae*. *Bioprocess Eng.* **7**(5), 225–228 (1992).
140. Mata-Sandoval, J. C., Karns, J. & Torrents, A. Effect of nutritional and environmental conditions on the production and composition of rhamnolipids by *P. aeruginosa* UG2. *Microbiol. Res.* **155**(4), 249–256 (2001).
141. Dahrazma, B., Mulligan, C. N. & Nieh, M.-P. Effects of additives on the structure of rhamnolipid (biosurfactant): A small-angle neutron scattering (SANS) study. *J. Colloid Interface Sci.* **319**(2), 590–593 (2008).
142. Lin, T. L., Chen, S. H., Gabriel, N. E. & Roberts, M. F. Small-angle neutron-scattering study of triglyceride solubilization by lecithin micelles: A direct observation of rod-to-sphere transition. *J. Phys. Chem.* **94**(2), 855–862 (1990).
143. Hamilton, J. A. & Small, D. M. Solubilization and localization of triolein in phosphatidylcholine bilayers: A 13C NMR study. *Proc. Natl Acad. Sci.* **78**(11), 6878–6882 (1981).
144. İkizler, B. *et al.* Surface adsorption and spontaneous aggregation of rhamnolipid mixtures in aqueous solutions. *Colloids Surf. A Physicochem. Eng. Asp.* **519**, 125–136 (2017).
145. Wu, L.-M. *et al.* Comparative studies on the surface/interface properties and aggregation behavior of mono-rhamnolipid and di-rhamnolipid. *Colloids Surf. B Biointerfaces* **181**, 593–601 (2019).
146. Kobierski, J., Wnętrzak, A., Chachaj-Brekiesz, A. & Dynarowicz-Latka, P. Predicting the packing parameter for lipids in monolayers with the use of molecular dynamics. *Colloids Surf. B Biointerfaces* **211**, 112298 (2022).
147. Ishigami, Y. *et al.* The pH-sensitive conversion of molecular aggregates of rhamnolipid biosurfactant. *Chem. Lett.* **16**(5), 763–766 (1987).
148. Lebrón-Paler, A. *et al.* Determination of the acid dissociation constant of the biosurfactant monorhamnolipid in aqueous solution by potentiometric and spectroscopic methods. *Anal. Chem.* **78**(22), 7649–7658 (2006).
149. Luning Prak, D. J., Abriola, L. M., Weber, W. J., Bocskay, K. A. & Pennell, K. D. Solubilization rates of n-alkanes in micellar solutions of nonionic surfactants. *Environ. Sci. Technol.* **34**(3), 476–482 (2000).
150. Myers, D. *Surfaces, Interfaces, and Colloids* (Wiley-Vch, 1999).
151. Gadaleta, D., Mangiatordi, G. F., Catto, M., Carotti, A. & Nicolotti, O. Applicability domain for QSAR models: Where theory meets reality. *Int. J. Quant. Struct.-Prop. Relatsh (IJQSPR)* **1**(1), 45–63 (2016).
152. Yu, H., Huang, G., Wei, J. & An, C. Solubilization of mixed polycyclic aromatic hydrocarbons through a rhamnolipid biosurfactant. *J. Environ. Qual.* **40**(2), 477–483 (2011).
153. E. Parliament, Regulation (EC) No 1907/2006 of the European Parliament and of the Council of 18 December 2006 concerning the Registration, Evaluation, Authorisation and Restriction of Chemicals (REACH), establishing a European Chemicals Agency, amending Directive 1999/45/EC and repealing Council Regulation (EEC) No 793/93 and Commission Regulation (EC) No 1488/94 as well as Council Directive 76/769/EEC and Commission Directives 91/155/EEC, 93/67/EEC, 93/105/EC and 2000/21/EC, in: E. Parliament (Ed.) 1907, 2006.

Acknowledgements

This work was partially funded by National Science Centre (Poland) through MINIATURA 1 grant no. 2017/01/X/ST5/02077 and co-funded by internal grant of Gdańsk University of Technology (DS/032403T016). The authors kindly acknowledge Polygen (Gliwice, Poland) for providing the UHPLC system (Dionex UltiMate 3000) equipped with Corona Veo RS and UV-VIS/DAD detectors for conducting part of this research. The authors also acknowledge Małgorzata Lesiuk and Paweł Czajerek from Polygen for their help in performing HPLC analyses, and Krystyna Rybicka and Małgorzata Borecka for their technical assistance.

Author contributions

Conception of the work: I.K-Ch., C.J. Design of the work: I.K-Ch., A.M., C.J. Funding acquisition: I.K-Ch. Literature data acquisition: I.K-Ch., P.M. RP-UHPLC-CAD/UV–VIS/DAD methodology and supervision: K.P. HPLC-Q-TOF–MS methodology and supervision: W.H-B. Experimental data acquisition: I.K-Ch., P.M., S.S., I.P. Data management and interpretation: I.K-Ch., A.M., C.J. Writing manuscript: I.K-Ch., C.J. Figures: I.K-Ch., A.M. Supplementary information: I.K-Ch. Critical review of the manuscript: A.M. Supervision: I.K-Ch. All authors reviewed the manuscript and have given approval to the final version of the manuscript.

Competing interests

The authors declare no competing interests.

Additional information

Supplementary Information The online version contains supplementary material available at https://doi.org/10.1038/s41598-024-59021-7.

Correspondence and requests for materials should be addressed to I.E.K.-C.

Reprints and permissions information is available at www.nature.com/reprints.

Publisher's note Springer Nature remains neutral with regard to jurisdictional claims in published maps and institutional affiliations.